ACS Infectious Diseases

Albright College

Subscriber access provided by ALBRIGHT COLLEGE

Article

Anti-schistosomal properties of Sclareol and its Heck-coupled derivatives: design, synthesis, biological evaluation and untargeted metabolomics

Alessandra Crusco, Helen Whiteland, Rafael Baptista, Josephine E. Forde-Thomas, Manfred Beckmann, Luis A.J. Mur, Robert J Nash, Andrew D. Westwell, and Karl F. Hoffmann

ACS Infect. Dis., **Just Accepted Manuscript** • DOI: 10.1021/acsinfecdis.9b00034 • Publication Date (Web): 13 May 2019

ACS Publications

is published by the American Chemical Society. 1155 Sixteenth Street N.W., Washington, DC 20036

Anti-schistosomal properties of Sclareol and its Heck-coupled derivatives: design, synthesis, biological evaluation and untargeted metabolomics

Alessandra Crusco [a,b], Helen Whiteland [a], Rafael Baptista [a], Josephine E. Forde-Thomas [a], Manfred Beckmann [a], Luis A. J. Mur [a], Robert J. Nash [c], Andrew D. Westwell [b*] and Karl F. Hoffmann [a*]

[a] Institute of Biological, Environmental and Rural Sciences (IBERS), Penglais Campus, Aberystwyth University, Aberystwyth SY23 3DA, United Kingdom

[b] School of Pharmacy and Pharmaceutical Sciences, Cardiff University, Cardiff CF10 3NB, United Kingdom

[c] PhytoQuest Limited, Plas Gogerddan, Aberystwyth, Ceredigion SY23 3EB Wales, UK

* Authors for correspondence:

KFH, e-mail: krh@aber.ac.uk

ADW, e-mail: WestwellA@cf.ac.uk,

Sclareol, a plant-derived diterpenoid widely used as a fragrance and flavouring substance, is well known for its promising antimicrobial and anticancer properties. However, its activity on helminth parasites has not been previously reported. Here, we show that sclareol is active against larval (IC_{50} ≈ 13 μM), juvenile (IC_{50} = 5.0 μM) and adult (IC_{50} = 19.3 μM) stages of *Schistosoma mansoni*, a parasitic trematode responsible for the neglected tropical disease schistosomiasis. Microwave-assisted synthesis of Heck-coupled derivatives improved activity, with the substituents choice guided by the Matsy decision tree. The most active derivative **12** showed improved potency and selectivity on larval (IC_{50} ≈ 2.2 μM, SI ≈ 22 in comparison to HepG2 cells), juvenile (IC_{50} = 1.7 μM, SI = 28.8) and adult schistosomes (IC_{50} = 9.4 μM, SI = 5.2). Scanning electron microscopy studies revealed that compound **12** induced blebbing of the adult worm surface at sub-lethal concentration (12.5 μM); moreover, the compound inhibited egg production at the lowest concentration tested (3.13 μM). The observed phenotype and data obtained by untargeted metabolomics suggested that compound **12** affects membrane lipid homeostasis by interfering with arachidonic acid metabolism. The same methodology applied to praziquantel (PZQ)-treated worms revealed sugar metabolism alterations that could be ascribed to previously reported action of PZQ on serotonin signalling and/or effects on glycolysis. Importantly, our data suggest that compound **12** and PZQ exert different anti-schistosomal activities. More studies will be necessary to confirm the generated hypothesis and to progress the development of more potent anti-schistosomal sclareol derivatives.

Keywords: diterpenoids, schistosomiasis, anthelmintic, sclareol, microwave synthesis, untargeted metabolomics

Sclareol is a labdane diterpenoid widely used as a fragrance[1] as well as a food flavouring substance[2] and is generally considered safe for topical and oral administration.[3] Originally isolated from *Salvia sclarea*, sclareol is also found in essential oils derived from other *Salvia spp* which are thought to be produced in response to infection by bacteria and fungi.[4] These plant-defence properties have led to further mechanistic investigations, which have demonstrated sclareol's potency as an antibacterial,[5] antifungal[6] and anticancer agent.[7–10] However, to the best of our knowledge, the activity of sclareol against parasitic helminths has not been previously investigated. As part of our ongoing efforts in identifying and characterising anthelmintic phytochemicals, we now report the activity of sclareol and new synthetic analogues against the causative helminth responsible for schistosomiasis.

Schistosomiasis is a chronic, debilitating helminthiasis caused by parasitic trematodes within the genus *Schistosoma* and currently affects approximately 600 million people.[11] This disease is predominantly found in tropical areas of the world and, with up to 300,000 deaths per year, is considered the most deadly neglected tropical disease (NTD).[12] In the absence of a prophylactic vaccine, schistosomiasis is primarily controlled by a single drug, praziquantel (PZQ). This pyrazino-isoquinolone is active against the adult stages of all human-infective *Schistosoma spp*, but not on immature forms and, therefore, requires repeat administrations to maximise efficacy.[13] Furthermore, the fear of selecting for PZQ insensitive or resistant parasites drives the need to identify new anti-schistosomal drugs with a different mechanism of action to PZQ. The identification of such compounds will contribute to the sustainable control of schistosomiasis into the future.[14]

Towards this end, several diterpenoids with anti-schistosomal activity have been previously reported,[15–17] including several from our group.[18,19] The collective results of these investigations demonstrate that this molecule class could be a promising source of next generation anthelmintic. In this study, the anti-schistosomal activity of sclareol was demonstrated on larval, juvenile and adult stages of *Schistosoma mansoni* and this activity was considerably improved

by the creation and testing of semi-synthetic derivatives. Based on initial structural-activity relationships (SARs) derived from a first group of analogues, different Heck-coupled derivatives were synthesised based on a previously reported synthetic route[20] and significantly improved by microwave-assisted synthesis. The choice of substituents was guided by the Matsy decision tree,[21] an updated version of the more classical Topliss scheme.[22] This process led to the synthesis of the most active compound **12** (IC_{50} ≈ 2.2 μM for schistosome larvae, SI > 20 in comparison to HepG2 cells; IC_{50} = 1.7 μM for juveniles, SI = 28.8; IC_{50} = 9.4 μM for schistosome adults, SI = 5.2). The effects of compound **12** on schistosome phenotype were investigated by Scanning Electron Microscopy (SEM), revealing tegumental alterations at a sub-lethal dose, characterised by swelling and bubble-like protrusions. Untargeted metabolomics of treated adult worms revealed significant alterations in lipid balance and, in particular, arachidonic acid (ARA) metabolism. These results are consistent with the previously reported effects of ARA on schistosome surface membranes.[23] Furthermore, the effect of compound **12** on schistosome metabolism is quite distinct to that induced by PZQ where alteration of sugar metabolism was predominantly observed. This metabolomics profile adds mechanistic support to the activity of PZQ in modulating serotonin signalling[24,25] and/or glycolysis[25,26] in schistosomes. The overall results of sclareol derivative synthesis, bioactivities and mechanism of action investigations (distinct from PZQ) are presented and discussed here.

RESULTS AND DISCUSSION

Anthelmintic activity of (-)-sclareol.

The activity of a small collection of plant-derived diterpenoids (see Supplementary Information, S1) on *S. mansoni* schistosomula (larvae), using the high throughput screening platform Roboworm,[18,27] identified anthelmintic properties among labdane-type diterpenoids. Based on this finding, we decided to ascertain the anthelmintic activity of enantiopure (-)-sclareol (Figure 1), the commercially available labdane diterpenoid (Figure 1A) more structurally-related to the labdane hits in S1 (same condensed rings, open chain and allylic alcohol group) and widely used in the cosmetic[1] and food[2] industries due to its excellent safety profile. Indeed, *in vivo* toxicity studies in mice have demonstrated a LD_{50} > 5000 mg/kg for both topical and oral delivery routes and a LD_{50} = 1000 mg/kg for the parental route.[3] Moreover, as sclareol is also well known for its promising antimicrobial and antifungal activities,[5,6] we postulated that this labdane diterpenoid possessed biological properties (low toxicity and anti-infective nature) to warrant anthelmintic investigations. Therefore, sclareol's ability to affect motility and phenotype of *S. mansoni* schistosomula was first assessed (final concentrations of 50 - 1 μM) by the Roboworm platform[18,27] (Figure 1B). Here, this diterpenoid demonstrated a dose-dependent anti-schistosomal activity with an IC_{50} of 14.2 μM for phenotype and 12.3 μM for motility (Figure 1B, 1F). Sclareol was then screened against juvenile (final concentrations of 50 - 0.8 μM) and adult worms (final concentrations of 50 - 3.13 μM) where it negatively affected worm motility (IC_{50} of 5.0 and 19.3 μM respectively) (Figure 1C, 1D, 1F) and inhibited production of the pathogenic eggs at the lowest concentration tested (Figure 1E). We additionally confirmed the low toxicity of sclareol[3] on human HepG2 cells (CC_{50} = 74.1 μM) (Figure 1F). Considering the relative low toxicity of sclareol, we decided to pursue further medicinal chemistry studies on this diterpenoid to improve its anthelmintic characteristics.

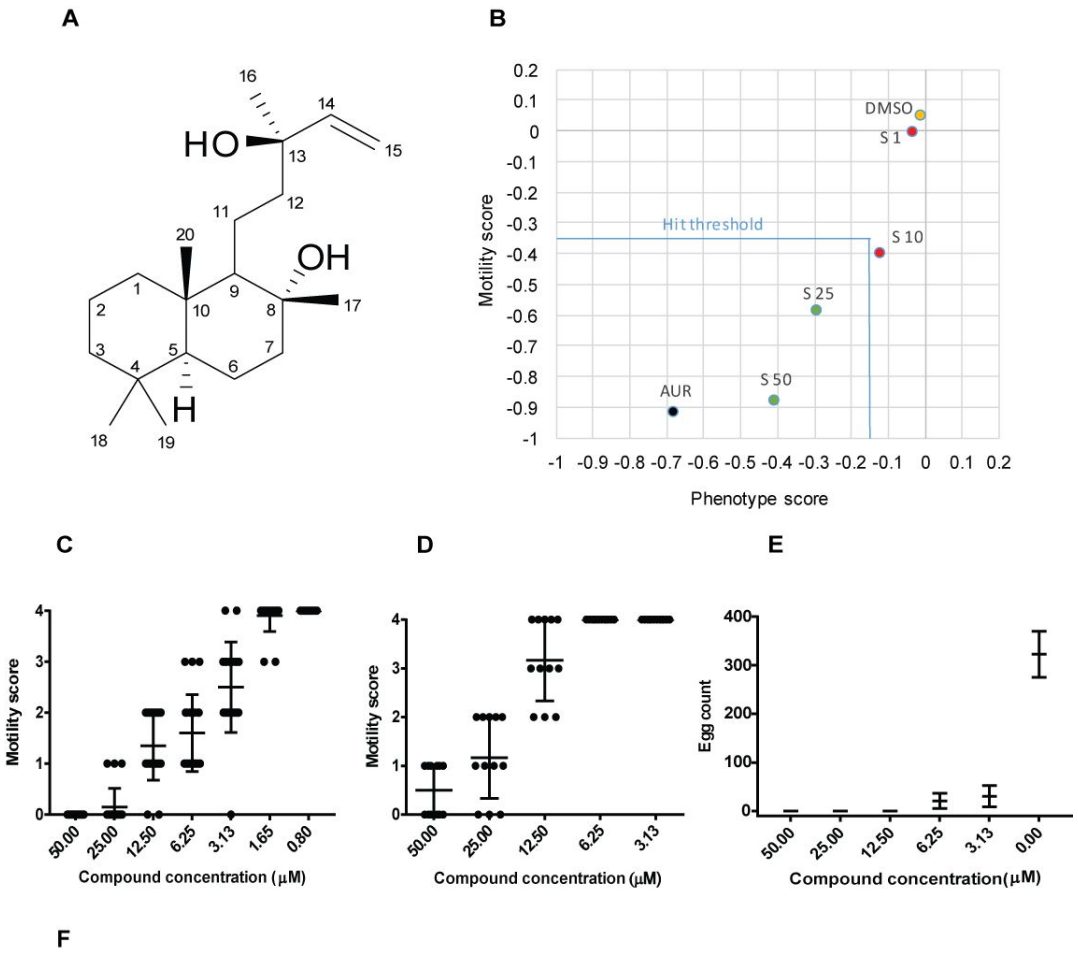

F

Compounds	IC_{50} on schistosomula phenotype / motility (µM)	IC_{50} on juvenile worms (µM)	IC_{50} on adult worms (µM)	CC_{50} on HepG2 cells (µM)	SI on schistosomula phenotype / motility	SI on juvenile worms	SI on adult worms
Sclareol	14.2 / 12.3	5.5	19.3	74.1	5.2 / 5.9	13.5	3.8

Figure 1. Structure and anti-schistosomal activity of (-)-sclareol. A) Structure and scaffold numbering system of the diterpenoid (-)-sclareol. B) Sclareol affects the phenotype and motility of *S. mansoni* schistosomula in a dose dependent manner (50 - 1 µM). Schistosomula co-cultivated with negative (0.625 % DMSO) and positive (Auranofin 10 µM, 0.625% DMSO) controls are also indicated. The screening was performed by the high throughput screening platform Roboworm[18,27] with each point being the average of two replicates (each replicate contains 120 parasites/well). Hit compounds (within the hit threshold) affect ≥ 70% of the larvae. Z'-scores[28]: 0.69 for phenotype and 0.48 for motility. C) Sclareol affects the motility of mixed-sex *S. mansoni* juvenile worms in a dose dependent manner (50 – 0.8 µM) and of D) mixed-sex *S. mansoni* adult worms (50 - 3.13 µM). Scores were calculated according to the Methods. Each point represents a single worm (10 juveniles x 2 independent experiments, 3 worm pairs x 2 independent experiments) with mean +/- SD illustrated. E) Sclareol inhibits egg production of *S. mansoni* adult worm couples when compared to control treatment (0.00). Values are mean +/- SD of egg counts from 3 worm pairs x 2 independent experiments. F) Estimated IC_{50}s (µM) calculated from dose response curves on schistosomula phenotype and motility, on juvenile and adult worm motility, estimated CC_{50} on HepG2 human liver cell and Selectivity Index (SI).

Synthesis of sclareol derivatives

To quantify structural activity relationships and improve upon the moderate anthelmintic activity of sclareol, a small group of analogues was first synthesised (Figure 2). Oxidation of sclareol with $KMnO_4$ and $MgSO_4$ in acetone[29] led to the synthesis of compound **1**, with the allylic alcohol substituted by a keto group. Dehydration of compound **1** with I_2 in toluene[29] led to compound **2**. A further derivative of sclareol was obtained by acetylation of both alcoholic functions by acetyl chloride in the presence of N,N-dimethylaniline in dichloromethane,[30] giving compound **3**, and subsequent selective hydrolysis by KOH in ethanol[30] leading to compound **4**. The latter, was subjected to an E1 elimination by using $NaHCO_3$ in DMSO, as described by Rogachev *et al.,*[30] with some modifications using microwave conditions (200 °C, 100 W, 11 min); this procedure led to the synthesis of compound **5** as a geometric isomeric mixture (2:1 exo:endo isomer mixture, as determined by ^{1}H-NMR integration, see Supplementary information, S2). The obtained dehydrated derivative was subjected to the Heck-reaction,[20] with yields and reaction times improved by microwave conditions (130°C, 300 W, 12 min), leading to compound **6**. The same Heck-reaction was performed directly on sclareol, obtaining the direct derivative compound **7**.

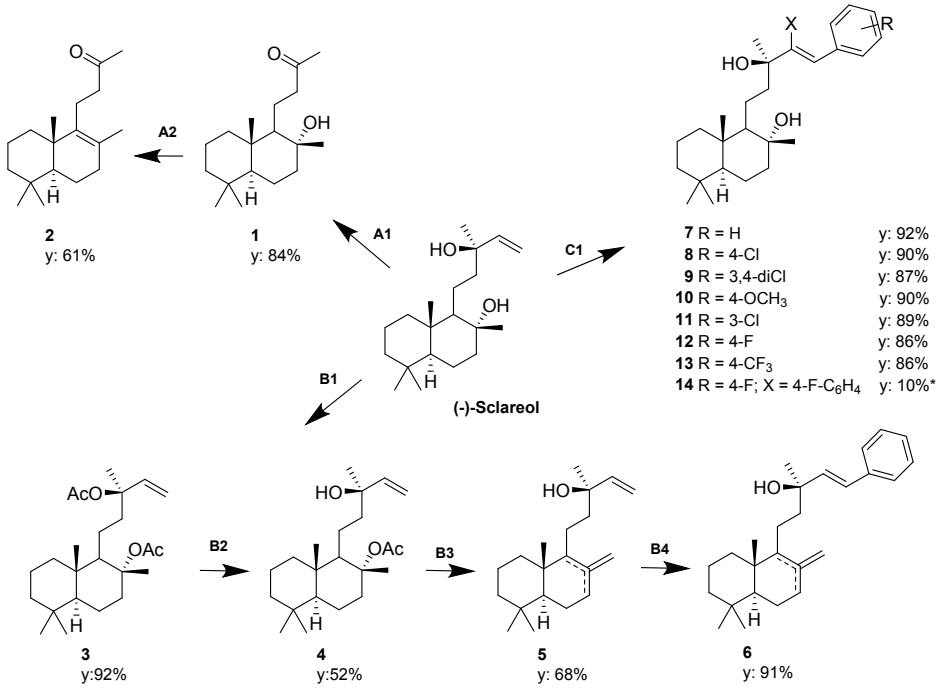

A1: $KMnO_4$ / $MgSO_4$ / acetone / rt / overnight **A2**: I_2 / toluene / reflux / 3 h **B1**: AcCl / N,N-DMA / DCM / rt / 24 h **B2**: KOH / H_2O / EtOH / rt / 24 h **B3**: $NaHCO_3$ / DMSO / 100 W / 200 °C / 11 min (microwave-assisted) **B4 = C1**: Ar-$B(OH)_2$ / $Pd(OAc)_2$ / $Cu(OAc)_2$ / NaOAc / DMF / 130 °C / 300 W / 12 min (microwave-assisted; *classic thermal for **14** at 80°C, 6 h). y = yield.

Figure 2. Derivatives of sclareol. Structures and synthetic scheme of the sclareol derivatives. When not specified, X = H.

To investigate the impact of these changes on anthelmintic activity, this first small set of compounds (**1** - **7**) was screened against the schistosomula stage of *S. mansoni*. Compounds **1** and **2** lost their potency (Table 1), showing that the allylic portion is important for anthelmintic activity. The *bis*-acetylated compound **3** was inactive too, while the mono-acetylated compound **4** recovered activity, comparable to sclareol, showing again that the free allylic alcohol is essential. The importance of the allylic alcohol for activity was also confirmed by comparison with the previous diterpenoid collection screening results (see Supplementary information, S1), where the two hit compounds **S6** and **S8** share this feature, while similar compounds presenting an inverted allylic alcohol (**S2**, **S10**) or replacement of the function (**S3**, **S9**) were not active. Compound **5** showed comparable activity to compound **4** (and to its plant-derived reference **S6**), while the addition of a phenyl ring in position 15 led to loss of activity in compound **6**.

Interestingly, this did not happen when the addition was made directly on sclareol to obtain compound **7**, which showed an almost 3-fold improved activity (IC_{50} ≈ 5.5 μM) over sclareol. Thus, we decided to pursue the synthesis of new Heck-coupled derivatives (compounds **7** - **13**) with different phenyl substituents. The previous described synthesis route,[20] using $Pd(OAc)_2$, $Cu(OAc)_2$, NaOAc in DMF at 80 °C, was followed and improved by microwave heating at 130 °C, leading to improved yields (from ~ 60% to ~ 90%) and improved reaction times (from 3 - 6 h to 11 min). Under microwave conditions, mono-coupled products (**7** - **13**) with *trans* configuration, as shown by the ^{1}H-NMR coupling constants of the alkene (J ≈ 16 Hz), were obtained; when using classic thermal synthesis, Heck-coupling led to the *bis*-arylated products (**14**) in addition to mono-coupled product (**12**).

To maximise the chance of finding more potent analogues against schistosomula while reducing the number of synthesis steps, the Matsy decision tree,[21] an updated version of the classical Topliss tree,[22] was followed (Figure 3). The first phenyl ring substitution with chlorine in the 4-position (compound **8**) improved anti-schistosomula activity of compound **7** to an IC_{50} ≈ 3.5 μM. The 3,4-dichloro-substituted compound **9** was then synthesised as suggested by the Matsy tree, but this led to decreased activity. Subsequently, the far right branch of the tree was followed, leading to the synthesis of 4-OMe (compound **10**) and 3-Cl (compound **11**) substituted analogues (the first with a solubility problem, the second with lower activity) as well as a 4-F analogue (compound **12**), which showed the most potent activity (IC_{50} ≈ 2.2 μM, 6-fold more potent than sclareol). Taking into account the increased activity brought by the fluorine group, a 4-CF_3 derivative was also synthesised (compound **13**); the double addition side product generated from the classical reaction of compound **12** (compound **14**) was also tested. While compound **13** was less potent, the activity of the side product (compound **14**) was more potent (IC_{50} ≈ 1.3 μM). The greater anti-schistosomula activity associated with the double addition side product **14** could be correlated with increased lipophilia compared to the correspondent single addition product **12**, which in turn is more lipophilic and potent when compared to sclareol

lacking a phenyl ring (calculated logP 7.9 > 6.4 > 4.7, respectively). Indeed, increased lipophilia could be responsible for a greater passage of the compound through the schistosomula membrane and, therefore, for better activity. However, changes in lipophilia brought about by phenyl substituents did not always follow this correlation (e.g. **8** is more potent than **9**, although calculated logP are 6.8 and 7.4, respectively) and suggest that other factors likely contribute. However, when compounds were tested on juvenile and adult worms, as fully described in the next paragraph, compound **12** was the most potent.

Table 1. Anti-schistosomal and HepG2 cytotoxicity activities

Compounds	IC_{50} on schistosomula phenotype / motility (μM)	IC_{50} on juvenile worms (μM)	IC_{50} on adult worms (μM)	CC_{50} on HepG2 cells (μM)	SI on schistosomula phenotype / motility	SI on juvenile worms	SI on adult worms
Sclareol	14.2 / 12.3	5.5	19.3	74.1	5.2 / 5.9	13.5	3.8
1	>25	NA	NA	>100	NA	NA	NA
2	>25	NA	NA	>100	NA	NA	NA
3	>25	NA	NA	>100	NA	NA	NA
4	11.6 / 12.1	NA	NA	>100	NA	NA	NA
5	12.9 / 10.4	NA	NA	85.1	6.6 / 8.2	NA	NA
6	>25	NA	NA	74.1	NA	NA	NA
7	5.7 / 5.3	2.0	18.6	43.7	7.7 / 8.2	21.9	2.3
8	3.5 / 3.6	6.5	12.7	42.7	12.2 / 11.9	6.7	3.4
9	27.6 / 10.6	NA	NA	93.3	3.4 / 8.8	NA	NA
10 *	>25	NA	NA	>100	NA	NA	NA
11	8.2 / 5.4	11.2	27.7	53.7	6.5 / 9.9	4.8	1.9
12	2.1 / 2.3	1.7	9.4	49.0	23.3 / 21.3	28.8	5.2
13	26.0 / 19.8	NA	NA	63.1	2.4 / 3.2	NA	NA
14	1.4 / 1.3	6.3	16.4	42.7	30.5 / 32.8	6.8	2.6

Estimated IC_{50}s (μM) calculated from dose response curves for *S. mansoni* schistosomula phenotype/motility and *S. mansoni* adult and juvenile worm motility. Estimated CC_{50}s (μM) calculated from dose response curves for HepG2 cells and Selectivity Indices (SI) of the anthelmintic activity when compared to the cell line. The values are mean results of experiments in duplicate for helminths or triplicate for cells (IC_{50}s and CC_{50}s with 95% confidence intervals in Supplementary Information, S3). * Solubility problem.

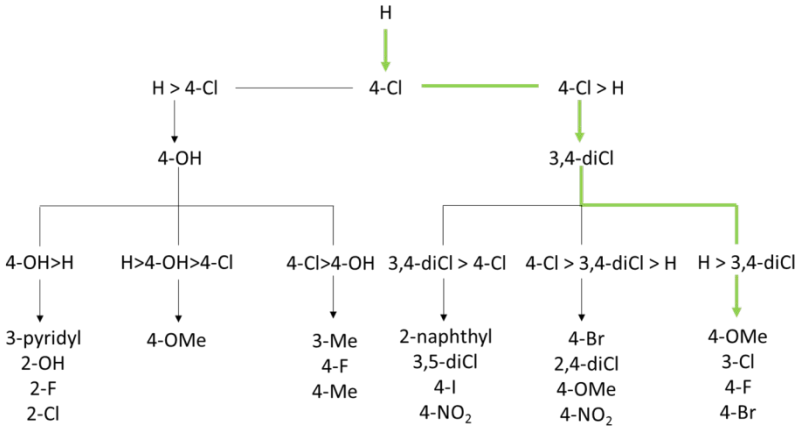

Figure 3. Matsy decision tree and pathway followed to generate more active anti-schistosomal compounds. The figure shows the Matsy decision tree by Boyle *et al.*,[21] an updated version of the classic Topliss decision tree. According to the increased or decreased activity brought by the different aromatic substituents, a pathway is followed leading to the choice of new substituents. The pathway followed in this study is highlighted in green.

Anthelmintic and cytotoxic screening of derivatives

As described above, to help inform the progression of hit compound identification, compounds were first titrated (50 to 1 μM) on *S. mansoni* schistosomula by using the automated platform Roboworm, which scores parasites based on their phenotype and motility.[18] A follow-on secondary screen of all synthesised compounds was subsequently completed to validate these results and to compare anti-schistosomal potency at 10 μM (Figure 4). In addition to this, all compounds were assessed for overt cytotoxicity by screening against the human HepG2 liver cell line (collective results shown in Table 1).

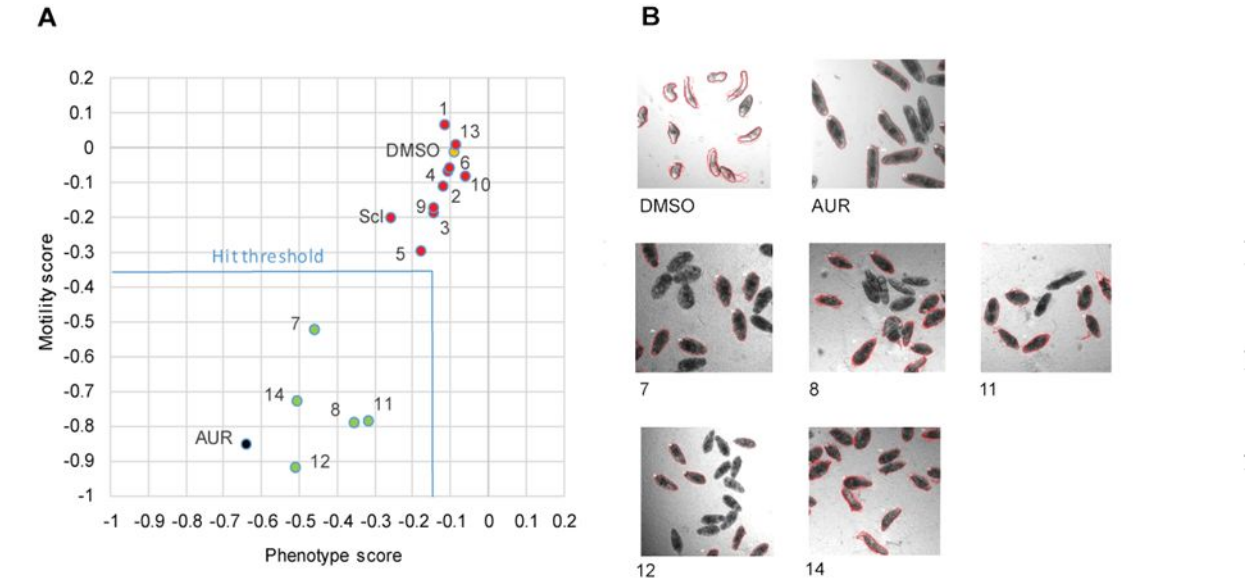

Figure 4. Screening of sclareol derivatives on *S. mansoni* schistosomula at 10 μM. A) The synthesised derivatives (at 10 μM) were assessed for their ability to affect phenotype and motility of *S. mansoni* schistosomula when compared to the original sclareol (Scl, 10 μM) as well as to the negative (0.625% DMSO) and positive (Auranofin 10 μM, 0.625% DMSO) controls. The screening was performed by the high throughput platform Roboworm as previously described.[18] Hit compounds (within the hit threshold) affect ≥ 70% of the larvae. Each point represents the average score of two replicates. Z'-scores[28]: 0.41 for phenotype and 0.23 for motility. B) Images of the parasites after treatment with the controls and the five hits at 10 μM are also shown. Control schistosomula presented a normal phenotype and high motility (indicated by change in red outlines), while affected schistosomula presented an altered phenotype (change in shape and darkening) and low or absent motility (no change in red outlines).

Compounds with IC_{50} values on schistosomula below 10 μM (**7**, **8**, **11**, **12** and **14**) were then selected for follow-on experiments against juvenile and adult schistosomes (Table 1; Supplementary information, S4 and S5). Similar to the anti-schistosomula screens, compound **12** showed the greatest activity (IC_{50} of 1.7 μM on juveniles, 9.4 μM on adults; Table 1) and inhibited egg production (despite worm recovery) at all concentrations tested (Figure 5).

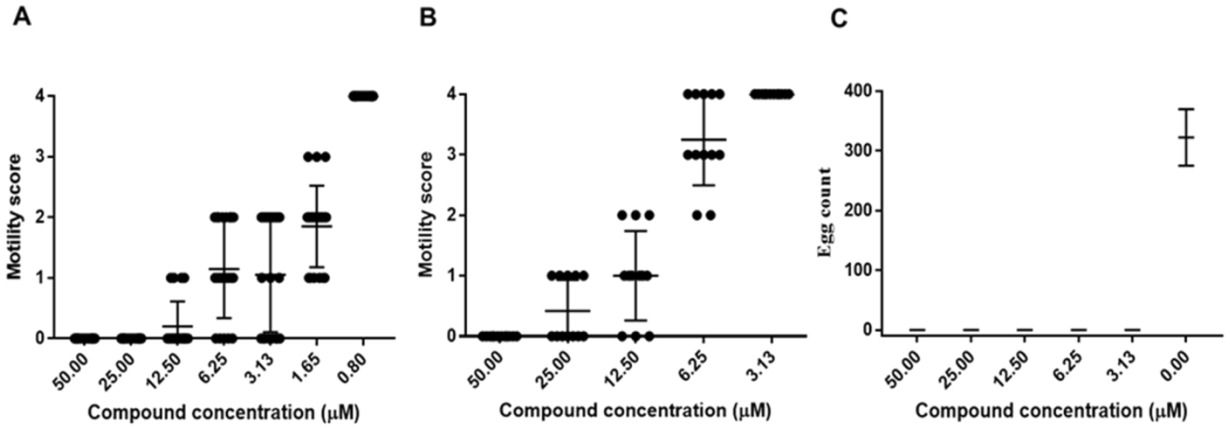

Figure 5. Screening of compound 12 on *S. mansoni* juvenile and adult worms. Compound **12** affects the motility of A) *S. mansoni* juvenile worms (50 – 0.8 μM) and B) *S. mansoni* adult worms (50 – 3.13 μM). Scores were calculated according to the Methods. Each point represents a single worm (10 juveniles x 2 independent experiments, 3 worm pairs x 2 independent experiments) with mean +/- SD shown. C) Compound **12** inhibits egg production (3 worm pairs/well x 2 replicate experiments) until the lowest concentration tested (3.13 μM) when compared to the DMSO control (0).

Phenotypes of adult worms treated with a sub-lethal concentration (12.5 μM) of compound **12** were analysed by SEM (Figure 6). The surface of treated parasites was altered when compared to the DMSO control and, in particular, blebbing, swelling of the tegument and bubble-like protrusions were observed on both male and female worms (Figure 6A and 6C compared to 6B and 6D). This suggested that the anti-schistosomal activity of compound **12** could be related to membrane or tegumental disruptions, as previously reported for other terpenoids.[16,17,31]

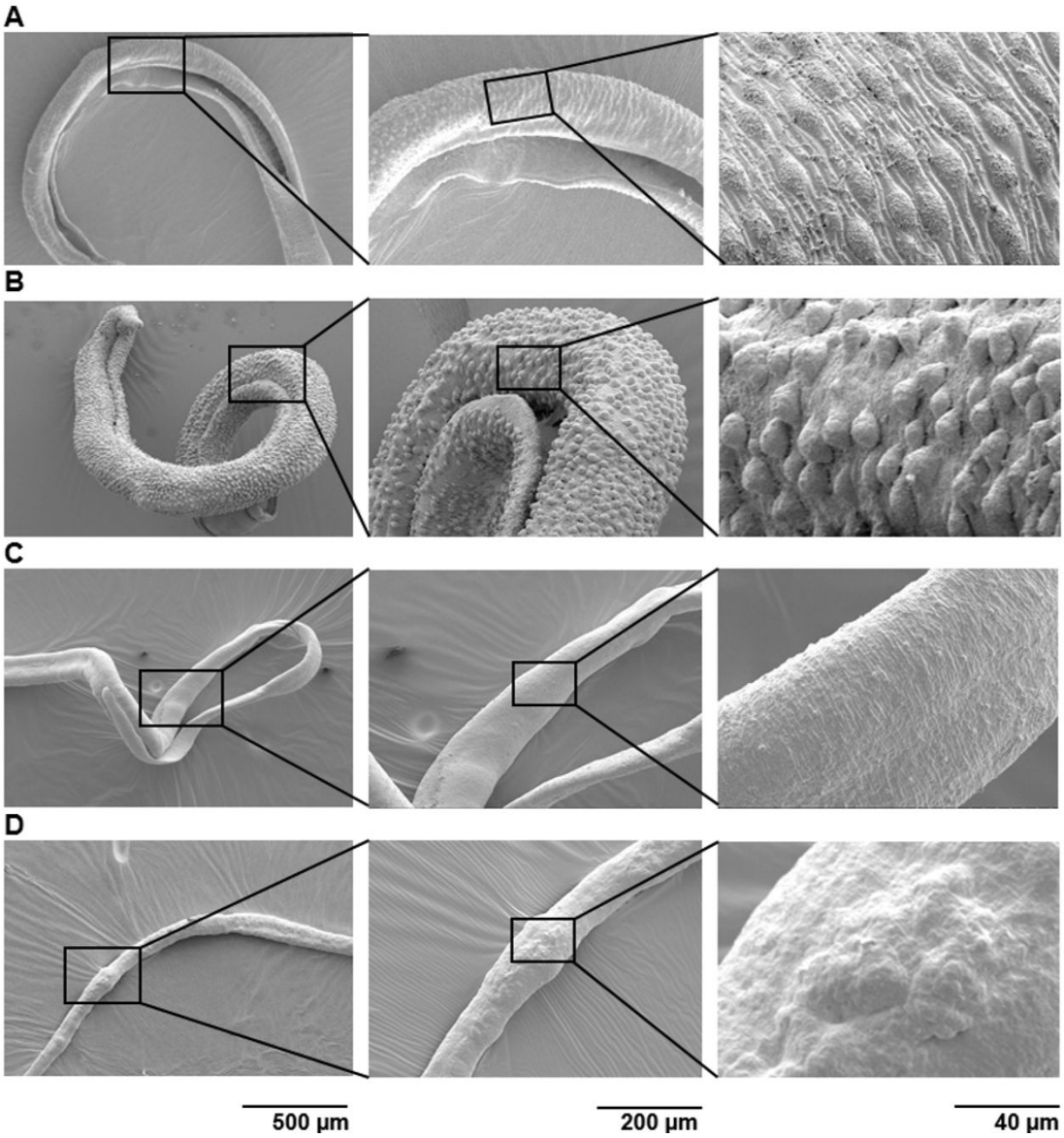

Figure 6. Scanning electron microscopy (SEM) images of *S. mansoni* worms co-cultivated with compound 12. SEM images of untreated adult male (A) and female (C) worms compared to male (B) and female (D) worms treated with compound **12** at 12.5 µM. The surface of the treated parasite appears damaged when compared to the control and the presence of bubble-like protrusions and swelling is evident.

Untargeted metabolomics

To further investigate the mode of action of compound **12**, analysis of metabolomic changes induced in adult worms co-cultured at its IC_{50} value was performed as described in the Methods, adapting the procedure applied on bacteria by Baptista et *al.*[32] and using MetaboAnalyst 4.0[33] for metabolite comparative quantification and annotation. Flow infusion electrospray ionisation high resolution mass spectrometry (FIE-HRMS) was used to profile extracted metabolites derived from treated (compound **12** vs PZQ) and control *S. mansoni* adult worms. Unsupervised principal component analysis (PCA) revealed that the metabolomics profile of worms treated with compound **12** is quite distinct from the metabolic profile of PZQ-treated and untreated worms, suggesting a different mode of action (Figure 7).

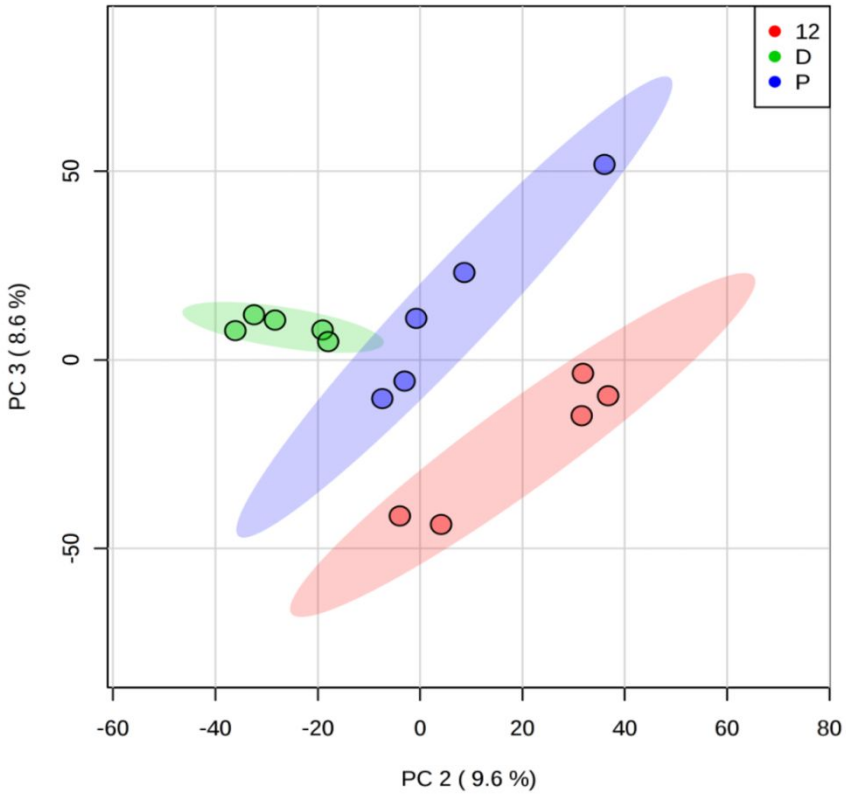

Figure 7. Principal component analysis (PCA) of *S. mansoni* adult worm metabolome. PCA score plots (positive and negative ionisation mode together, coloured regions display 95% confidence interval) of normalised *m/z* intensities of metabolites extracted from *S. mansoni* adult worms after 24 h treatment with compound **12** (12, in red) at IC_{50} concentration (9.4 μM) compared to worms treated with DMSO (0.625%) (D, in green) and to worms treated with PZQ (P, in blue) at IC_{50} concentration (30 nM; Supplementary Information, S6).

Metabolites responsible for separation between compound **12** treated and control worms (DMSO) in PCA were identified using MetaboAnalyst 4.0.[33] A total of 2123 *m/z* FIE-HRMS features were found to be significantly different ($p < 0.01$) between the two samples considering positive and negative ionisation mode together (1210 and 913, respectively). MetaboAnalyst 4.0 - MS peaks to pathway was used to identify these variables. The software used the *mummichog* algorithm, which allows avoidance of the *a priori* identification of metabolites and the biased manual assignment of spectral features to metabolites[34] by looking for local enrichment after plotting all possible matches in the metabolic network. This method provides accurate reproduction of true activity, as the false matches distribute randomly.[34] The run analysis revealed that arachidonic acid (ARA), pentose phosphate, pyrimidine, amino sugar and fructose and mannose metabolism were all significantly affected in compound **12** treated worms (Table 2A for significant pathways, Supplementary Data SD1-2 for all identified metabolites SD3-4 for all identified pathways).

Table 2. Significantly affected pathways in adult *S. mansoni* worms after 24h treatment with compound 12 and PZQ (compared to DMSO control worms)

A. Compound 12 vs control worms

	Pathway total	Hits tot.	Hits sig.	EASE	FET	Gamma
Arachidonic acid metabolism[a]	14	6	6	0.10996	0.01598	0.00013
Pentose phosphate pathway[b]	19	12	11	0.03670	0.00711	0.00008
Pyrimidine metabolism[b]	32	17	14	0.05077	0.01550	0.00009
Amino sugar and nucleotide sugar[b]	27	14	12	0.05509	0.01460	0.00009
Fructose and mannose metabolism[b]	16	10	9	0.09049	0.02083	0.00012

B. PZQ vs control worms

	Pathway total	Hits tot.	Hits sig.	EASE	FET	Gamma
Glycolysis or Gluconeogenesis[b]	25	15	14	0.03936	0.00830	0.00008
Citrate cycle (TCA cycle)[b]	20	10	10	0.06189	0.00890	0.00010

Fructose and mannose metabolism[b]	16	10	10	0.06189	0.00890	0.00010
Pentose and glucuronate interconversions[b]	11	9	9	0.09122	0.01435	0.00012
Pentose phosphate pathway[b]	19	12	11	0.11081	0.02864	0.00013
Alanine, aspartate and glutamate metabolism[b]	17	12	11	0.11081	0.02864	0.00013

a From metabolites identified in positive ionisation mode

b From metabolites identified in negative ionisation mode

Pathways identifications were performed by using MetaboAnalyst 4.0,[33] as described in the Methods section, after analysis and identification (tolerance = 3ppm) of *m/z* features obtained by high resolution mass spectrometry. The tables includes ranked enriched pathways, total number of hits, significant hits ($p < 0.05$), their EASE (Expression Analysis Systematic Explorer) score,[35] their raw *p*-values (Fisher's exact test, FET) and the *p*-values using a Gamma distribution.

Within the positive ionisation mode, the only pathway found to be significantly affected by compound **12** was ARA metabolism. Specifically, ARA and its downstream derivatives prostaglandin (PG) E2 and/or D2 were found in higher abundance within the metabolite pool of compound **12** treated worms when compared to controls (Figure 8A). Interestingly, exogenously administered or elevated levels of host derived ARA have previously been shown to kill schistosomes *in vitro* as well as *in vivo*.[23,36] Because of this and an excellent safety profile, ARA has recently undergone clinical trials in school children within highly endemic regions.[37,38] While ARA led to worm reductions similar to PZQ in both lightly- or heavily-infected children, it potentiated the effect of this anthelmintic when co-administrated to both study populations. The proposed mechanism of ARA action on schistosome viability has been reported to function through activation of the tegument-associated neutral sphingomyelinase, nSMase; this enzyme is responsible for sphingomyelin hydrolysis and a consequent increase in membrane permeability and alteration of lipid balance, as well as exposure of surface antigens to antibody binding.[23,38,39] Interestingly, the reported phenotype for ARA-treated worms includes tegumental disruption and the formation of "bubble-like lesions",[23] very similar to what was observed in compound **12** treated worms. Indeed, sphingomyelin hydrolysis is associated with internal release of ceramide,[40] signalling molecules that have been previously associated with

membrane blebbing and apoptosis.[41] Collectively, these observations seem to suggest that compound **12** affects schistosome survival by interfering with either ARA metabolism and/or PGE2/D2 homeostasis. Although PG-producing cyclooxygenases have not yet been identified in schistosomes,[42] prostaglandins are a major component of the schistosome lipidome[43] and are thought to be involved in host immune system evasion[44] as well as in cercarial penetration.[45] Whether these altered PGE2/PGD2 levels, induced by compound **12**, would also affect schistosome survival *in vivo* is currently unknown. However, this hypothesis seems plausible due to the importance of these downstream ARA products in modulating host interactions. Finally, and similar to the phenomenon observed for other diterpenoids on human cells,[46,47] the lipophilic structure of compound **12** may directly affect schistosome survival by altering PG and lipid balances essential for normal maintenance of the worm's heptalaminate barrier.

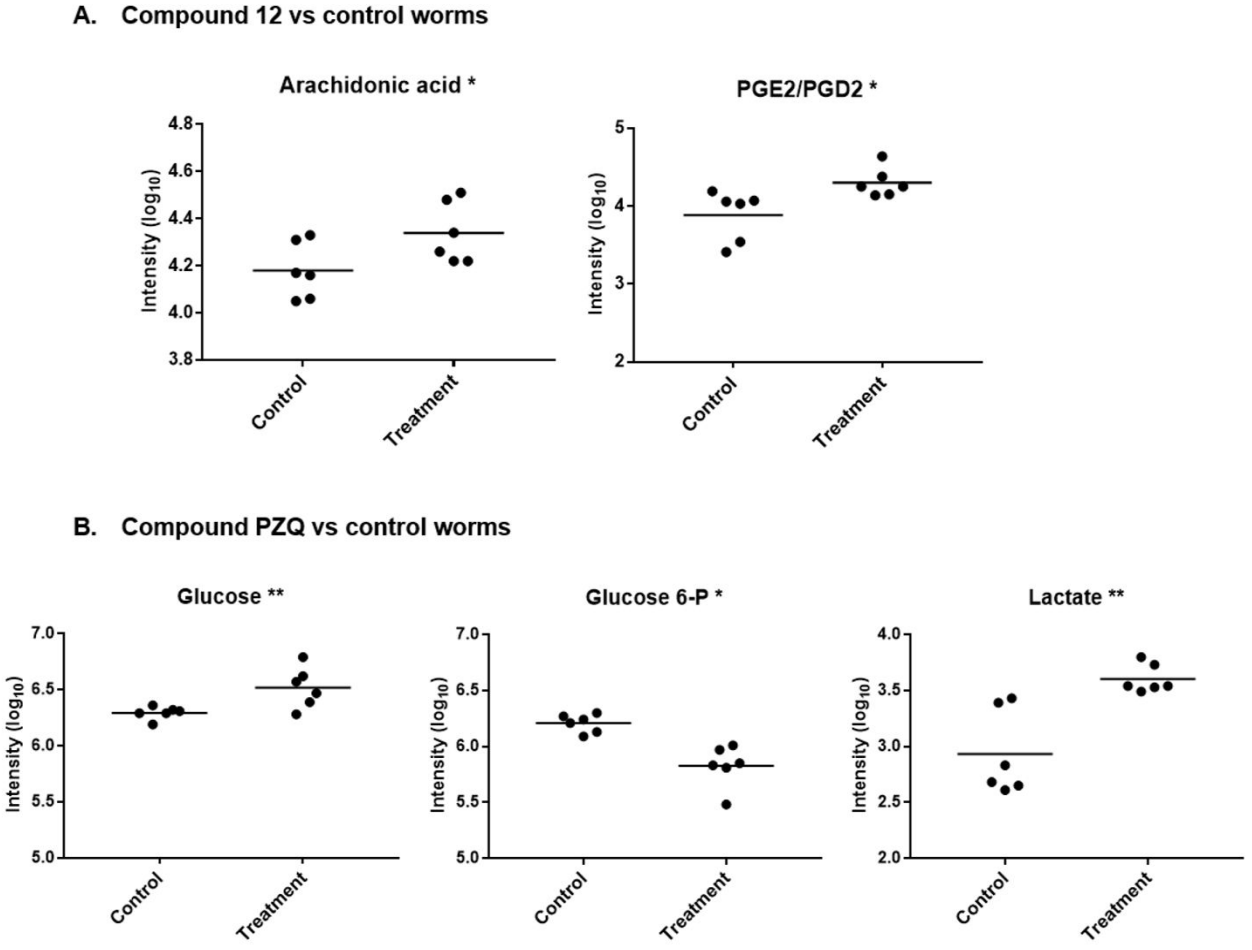

Figure 8. Significant affected key-metabolites found in treated schistosomes. Some key metabolites with significantly (*p < 0.01, **p < 0.001) different concentrations found between control and treatment. A) Compound **12** treatment induces increased production of arachidonic acid and prostaglandins (e.g. PGE2 or PGD2 level; as the two prostaglandins are structural isomers with the same exact mass and belonging to the same enriched pathway, the algorithm is not able to distinguish between them). B) PZQ-treatment induces increased production of glucose and lactate, while levels of glucose 6-phosphate were decreased.

When examining the compound **12** induced pathways significantly enriched in the negative ionisation mode, the involvement of sugar metabolism was evident. In particular, pentose phosphate pathway (PPP) metabolites were less abundant. As one of the main functions of the PPP is to generate metabolites essential for nucleic acid synthesis, it was not surprising that nucleotides and nucleotide sugars were also less abundant in compound **12** treated schistosomes. The other main function of the PPP is in the synthesis of NADPH that, in mammals, is necessary for fatty acid synthesis; therefore, the PPP would be downregulated when fatty acids are in abundance. Despite the lack of a proper *de novo* lipogenesis, schistosomes can synthesise new fatty acids by modification of host-derived ones using NADPH-dependent enzymes;[48] therefore, similar to mammals, we speculate that the PPP was likely downregulated in compound **12** treated worms due to the increase in abundance of fatty acids (here ARA).

To determine if these metabolomics changes are specific to compound **12** or are generally induced in schistosomes upon all anthelmintic stresses, interrogation of the metabolomics signatures between PZQ-treated and untreated worms was subsequently performed. To our knowledge, this has not been done before and may also represent a novel way of identifying PZQ's mechanism of action. A total of 2756 *m/z* HRMS features were found to be significantly different (p < 0.01) between the two samples considering positive and negative ionisation modes together (1725 and 1031, respectively). Affected pathways mainly belonged to sugar metabolism (i.e. glycolysis or gluconeogenesis), citrate cycle, fructose and mannose

metabolism, pentose and glucuronate interconversions, PPP and the metabolism of the glucogenic amino acids alanine, aspartate and glutamate (see Table 2B for significant pathways, Supplementary Data SD1-2 for all identified metabolites and SD5-6 for all identified pathways). In particular, the main product of schistosome carbohydrate metabolism, lactate, was found to be more abundant than in the control; other glucose pool metabolites (e.g. glucose 6-P) were found in decreased abundances, while glucose itself was found to be in much higher concentration (Figure 8B). Considering the recent report describing PZQ as a human serotonin 5-HT_{2b} receptor agonist,[24] we assessed how our metabolomics data paralleled serotonin pathway activation. In schistosomes, serotonin increases carbohydrate catabolism by increasing glycogen utilization, stimulating glycolysis and, therefore, increasing production of lactate.[49] Moreover, serotonin also causes an increase in glucose uptake.[49] Disturbance of carbohydrate metabolism, with an increase in glycogen breakdown, and an impairment of serotonin-stimulation of carbohydrate metabolism have also been described in PZQ-treated schistosomes.[25] All these previously reported effects are compatible with the observed data, supporting the idea that PZQ could alter serotonin signalling in schistosomes, too. A different hypothesis that could justify an increased glucose concentration, associated with a decreased concentration of glucose-6-phosphate, is a direct interference of PZQ in the glycolytic pathway. In schistosomes, the enzyme responsible for glucose phosphorylation is a hexokinase with intermediate characteristic between mammalian hexokinase and glucokinase and is a strong point of glycolysis regulation.[50] An antagonist effect of PZQ on hexokinase was recently demonstrated on the trematode *Clonorchis sinensis*,[26] whose hexokinase share 69% identity with *S. mansoni*. A similar antagonist action of PZQ on *S. mansoni* hexokinase would justify a decreased glucose phosphorylation. However, we cannot exclude that the observed effects on glycolysis could also be a consequence of generalised cellular stress.

CONCLUSIONS

In summary, we demonstrated that sclareol, a nontoxic diterpenoid widely used in the cosmetic and food industries, has anti-schistosomal properties. By pursuing the medicinal chemistry development of 14 derivatives, we have created more active compounds. The most potent derivative, compound **12,** showed a selective improved potency on larval schistosomes (IC_{50} ≈ 2.2 µM, SI ≈ 22 when compared to HepG2 cells), juveniles (IC_{50} = 1.1 µM, SI = 44.5) and adult worms (IC_{50} = 9.4 µM, SI = 5.2). Moreover, phenotypic analyses by SEM and metabolomics investigation revealed that this diterpenoid likely acts by disrupting surface membranes through alterations of ARA metabolism. This mechanism of action is quite distinct from that ascertained by metabolomics-based investigation of PZQ-treated worms, which revealed carbohydrate metabolism alterations similar to that observed upon serotonin signalling. Further mechanistic analyses of sclareol derivatives could provide important information for the development of novel anti-schistosomal molecules.

METHODS

Chemistry

Enantiomerically pure (-)-sclareol was purchased from Sigma Aldrich (357995-1G, CAS 515-03-7) and used without further purification. The diterpenoid small collection was obtained by PhytoQuest Ltd and all other reagents or solvents were obtained from Sigma Aldrich or Fisher Scientific and used without purification. The synthesised sclareol derivatives were characterized by high resolution mass spectrometry (HRMS), ^{1}H, ^{13}C and two-dimensional Nuclear Magnetic Resonance (NMR) spectroscopy (2D COSY, HSQC). NMR spectra were recorded on a Bruker Avance 500 MHz NMR spectrometer, with $CDCl_3$ used as solvent and NMR spectra referenced to the $CDCl_3$ residual peak. All the reactions were checked by Thin Layer Chromatography (TLC) on pre-coated TLC aluminium sheets of silica gel. All the synthesised derivatives were purified by column chromatography on silica gel (35-70 mesh) using the eluents indicated. Mass spectrometry was performed on an Orbitrap Fusion Thermo Scientific with a Dionex UltiMate 3000 UHPLC system. Microwave-assisted reactions were performed in a CEM discover microwave synthesiser 2005 (908010, serial number DU9667).

The general methods for synthesis and the characterization (^{1}H and ^{13}C NMR, HRMS) of all the synthesised compounds, as well as ^{1}H and ^{13}C NMR spectra of key compounds (**7**, **8**, **11**, **12** and **14**) can be found in the Supplementary Information.

Compound handling and storage

(-)-Sclareol and all the synthesised derivatives were solubilised in DMSO (Fisher Scientific, Loughborough, UK) and stored at -20°C at a stock concentration of 16 mM.

Schistosoma mansoni schistosomula culture and compound screening

S. mansoni (Puerto Rican Strain, Naval Medical Research Institute - NMRI) schistosomula were obtained by mechanical transformation[51] of *S. mansoni* cercariae collected after exposure of infected *Biomphalaria glabrata* (NMRI) snails to 2 h of light at 26 °C. Newly transformed schistosomula were deposited in 384-well black-sided microtiter plates (Perkin Elmer, MA, USA) and screened by the high throughput screening platform Roboworm as previously described,[18,27] with a final DMSO concentration of 0.625%. The effect of compounds on phenotype and motility of schistosomula was analyzed after 72 h using the image analysis model described by Paveley *et al.*[52] Phenotype and motility scores were used to calculate IC_{50} values derived from dose response titrations (50, 25, 10 and 1 μM) by using GraphPad Prism 7.02.

Schistosoma mansoni juvenile worm culture and compound screening

S. mansoni juvenile worms were recovered from hepatic portal veins by perfusion (Smithers and Terry, 1965) three weeks after percutaneous exposure of TO mice (Harlan, UK) to ~ 4000 *S. mansoni* cercariae and collected as previously described (Whiteland *et al.*, 2018). Briefly, collected worms were transferred into 50 mL falcon tubes and subjected to three series of centrifugation (300 x *g* for 2 min) and washing (in phenol-red free DMEM) steps, with the final washed parasites pelleted by gravity. Between ten and fifteen juvenile worms were cultured per well in a 96-well tissue culture plate (Fisher Scientific, Loughborough, UK). Each well contained 200 μL of modified DMEM (Gibco, Paisley, UK) supplemented with 10% v/v Hepes (Sigma-Aldrich, Gillingham, UK), 10% v/v Foetal Calf Serum (Gibco, Paisley, UK), 0.7% v/v 200 mM L-Glutamine (Gibco, Paisley, UK) and 1% v/v Antibiotic/antimycotic (Gibco, Paisley, UK). After incubation for 2 h at 37 °C in a humidified atmosphere containing 5% CO_2, test compounds were added to obtain the final concentrations of 50, 25, 12.5, 6.25, 3.13, 1.65 and 0.8 μM (0.3% DMSO final concentration). After 72 h, worms were scored manually using microscopic methods previously described (Whiteland *et al.*, 2018). Briefly, a score of 0 equaled no detectable movement, 1 included movement of the suckers and/or slight body contraction, 2 represented

slow movement of anterior and posterior regions, 3 equated to sluggish movement of the full body and 4 represented normal movement. IC_{50} values were determined using GraphPad Prism 7.02.

Schistosoma mansoni adult worm culture and compound screening

Mature adult parasites were recovered from hepatic portal veins by perfusion[53] seven weeks after percutaneous exposure of TO mice (Harlan, UK) to 180 *S. mansoni* cercariae. Three adult worm pairs were cultured per well in a 48-well tissue culture plate (Fisher Scientific, Loughborough, UK). Each well included 1 mL of modified DMEM (Gibco, Paisley, UK) media containing 10% v/v Hepes (Sigma-Aldrich, Gillingham, UK), 10% v/v Foetal Calf Serum (Gibco, Paisley, UK), 0.7% v/v 200 mM L-Glutamine (Gibco, Paisley, UK), 1% v/v Antibiotic/antimycotic (Gibco, Paisley, UK). After incubation for 2 h at 37 °C in a humidified atmosphere containing 5% CO_2, test compounds were added to obtain the final concentrations of 50, 25, 12.5, 6.25 and 3.13 μM (0.3% DMSO final concentration). After 72 h, worms were scored manually using microscopic methods described in the literature[54] and eggs collected and counted from each well. IC_{50} values were determined using GraphPad Prism 7.02.

HepG2 cell culture and MTT assay

HepG2 human liver cancer cells were grown to ~ 80% confluency in a modified BME culture media (containing 10% v/v Foetal Bovine Serum, 1% v/v MEM non-essential amino acid solution, 1% v/v 200 mM L-Glutamine, 1% v/v antibiotic/antimycotic). Confluent cells were subjected to cytotoxicity assays as previously described.[18,27] Briefly, 2.5 $x10^4$ cells per well were cultured in a black walled 96-well microtiter plate (Fisher Scientific, Loughborough, UK) and incubated for 24 h at 37 °C in a humidified atmosphere with 5% CO_2. Test compounds were then titrated from 100 to 3.13 μM (1.25 final % DMSO) and negative (DMSO; 1.25%) and

positive (1% v/v Triton X-100)[55] controls included. After 24 h incubation, the MTT assay was performed as described.[18,27] CC_{50} values were determined using GraphPad Prism 7.02.

Scanning Electron Microscopy (SEM)

Adult worms, cultured for 72 h with sub-lethal concentrations of test compounds and negative (DMSO) controls, were collected and prepared for SEM analysis. Several steps from Collins *et al*.[56] were adapted as previously described.[18] Briefly, collected schistosomes were relaxed in 1mL of anaesthetic (1% ethyl 3-aminobenzoate methane (Sigma-Aldrich, Gillingham, UK) dissolved in DMEM) and then killed in 1mL of 0.6mM $MgCl_2$ (Fisher Scientific, Loughborough, UK). After washing in PBS, worms were placed in SEM fixative (0.1M sodium cacodylate, 2.5% v/v glutaraldehyde (Agar Scientific, Stansted, UK) in ultra-pure water) and stored at 4°C until ready for SEM analysis. In preparation for SEM analysis, the stored samples were exposed to a number of wash, staining and dehydration steps as described[18] and finally mounted for the imaging. SEM analysis was conducted using a Hitachi S-4700 FESEM microscope (Ultra High Resolution, an accelerating voltage of 5.0kV with a working distance of 5.0 mm). Images were captured at 2560x1920 resolution.

Metabolomics sample preparation and metabolite extraction

The procedure previously described by Baptista *et al.*[32] was adapted to schistosome materials. Adult male worms were collected and cultured in media as described in previous paragraphs. In brief, 24-well plates were set up with 10 male worms per well (one biological replicate), for a total of 18 wells (6 replicates per 3 time points) per treatment (compound **12** and PZQ, at their respective IC_{50}, 9.4 μM and 30 nM, and control). At each time point (0, 12, 24 h), worms were removed from culture, immersed in liquid nitrogen to quench metabolism and stored at - 80 °C. In preparation for the extraction, samples were thawed, centrifuged (10 °C, 2000 rpm) and washed with phosphate buffer saline. Worms were disrupted by mill bead homogenizer and

extraction performed in chloroform/methanol/water 2:5:2 solution. After a final centrifugation, 100 µL of solution were transferred in mass vials for FIE-HRMS analysis.

Metabolomics analysis

Extracted metabolites were analysed by flow infusion electrospray ionisation high-resolution mass spectrometry (FIE-HRMS) in the High Resolution Metabolomics Laboratory (HRML), Aberystwyth University. FIE-HRMS was performed by a Q-Exactive Plus mass analyser equipped with an UltiMate 3000 UHPLC system, which includes Thermo-Scientific binary pump, column compartment (not used) and auto sampler. Metabolite fingerprints were created in both positive and negative polarity switching mode. Ion intensities were acquired between *m/z* 55 and 1200 for 3.5 min in profiling mode at a resolution setting of 280,000. 20 µl of each extracts were injected by auto sampler into a flow of 100 µl*min^{-1} methanol:water (70:30, v/v). Electrospray ionisation (ESI) source parameters were set in agreement with manufacturer's recommendations. An in-house data aligning routine in Matlab (R2013b, The MathWorks) was used to join mass spectra around the apex of the infusion maximum into a single mean intensity matrix (runs x *m/z*) for each ionisation mode. Data from the matrix were $\log_{10}$-transformed and used for statistical analysis performed by MetaboAnalyst 4.0. - Statistical analysis.[33] Metabolites and pathway identification were performed by MetaboAnalyst 4.0. - MS peaks to pathway[33] (tolerance = 3ppm, model organism = *S. mansoni*; time point = 24h, as this had the highest number of significantly different features). MetaboAnalyst identified pathways based on the *mummichog* algorithm, which predicts metabolome changes directly from mass spectrometry data, without the *a priori* identification of metabolites and avoiding the biased manual assignment of spectral features to metabolites [34]. *Mummichog* looks for local enrichment after plotting all possible matches in the metabolic network, providing accurate reproduction of true activity, as the false matches will distribute randomly.[34] Examples of key-

metabolites were analysed for significant difference (t-test) between control and treatment on Microsoft Excel and by GraphPad Prism 7.02.

Ethics statement

All procedures performed on mice adhered to the United Kingdom Home Office Animals (Scientific Procedures) Act of 1986 (project license PPL 40/3700) as well as the European Union Animals Directive 2010/63/EU and were approved by Aberystwyth University's (AU) Animal Welfare and Ethical Review Body (AWERB).

Author contribution

Conceived and designed the experiments: AC, ADW, KFH. Performed the experiments: AC (compound synthesis and characterization), AC (*S. mansoni* and HepG2 cell screening), RJN (providing plant-derived diterpenoids), HW (plant-derived diterpenoid screening), AC, RB, JEF, MB, LM (metabolomics). Manuscript preparation: AC (original draft), ADW, KFH (editing and revision).

Acknowledgment

We thank all of Prof. Karl F. Hoffmann's laboratory for help in maintaining the *S. mansoni* life cycle. We thank Prof. Andrea Brancale for the use of the microwave synthesiser.

Funding

We thank the Welsh Government, Life Sciences Research Network Wales scheme for financial support to AC and RB. IBERS receives strategic funding from the BBSRC.

The authors declare no competing financial interest.

Supplementary Information

Supplementary information include general methods for synthesis and characterization (^{1}H-NMR and ^{13}C-NMR peak lists, HRMS) of all the synthesized compounds, ^{1}H-NMR and ^{13}C-NMR spectra of key-compounds, screening of diterpenoid small collection on *S. mansoni* schistosomula, anti-schistosomal and cytotoxicity data summary (IC_{50} and CC_{50} with 95% confidence interval), scatter graphs for *S. mansoni* juvenile, adult worms and eggs count after treatments with key-compounds, PZQ titration on adult worms.

Supplementary Data Files

SD1: Identification (matched compounds as KEGG code) of metabolites found by positive ionisation mode.

SD2: Identification (matched compounds as KEGG code) of metabolites found by negative ionisation mode.

SD3: Ranked enriched pathways with total number of hits found by positive ionisation mode after compound **12** treatment, significant hits ($p < 0.05$), their EASE (Expression Analysis Systematic Explorer) score,[35] their raw *p*-values (Fisher's Exact Test, FET) and the *p*-values using a Gamma distribution.

SD4: Ranked enriched pathways with total number of hits found by negative ionisation mode after compound **12** treatment, significant hits ($p < 0.05$), their EASE (Expression Analysis Systematic Explorer) score,[35] their raw *p*-values (Fisher's Exact Test, FET) and the *p*-values using a Gamma distribution.

SD5: Ranked enriched pathways with total number of hits found by positive ionisation mode after PZQ-treatment, significant hits ($p < 0.05$), their EASE (Expression Analysis Systematic Explorer) score,[35] their raw *p*-values (Fisher's Exact Test, FET) and the *p*-values using a Gamma distribution.

SD6: Ranked enriched pathways with total number of hits found by negative ionisation mode after PZQ-treatment, significant hits ($p < 0.05$), their EASE (Expression Analysis Systematic Explorer) score,[35] their raw *p*-values (Fisher's Exact Test, FET) and the p-values using a Gamma distribution.

References

1. Caniard A., Zerbe P., Legrand S., Cohade A., Valot N. Discovery and functional characterization of two diterpene synthases for sclareol biosynthesis in *Salvia sclarea* (L.) and their relevance for perfume manufacture. *BMC Plant Biol*. 2012;**12**(1):1. Doi: 10.1186/1471-2229-12-119.
2. Smith RL., Waddell WJ., Cohen SM., Feron VJ., Marnett LJ., Portoghese PS., Rietjens IMCM., Adams TB., Gavin CL., Mcgowen MM., Taylor S V., Williams MC. GRAS 24: the 24th publication by the FEMA Expert Panel presents safety and usage data on 236 new generally recognized as safe flavoring ingredients. *Food Technol*. 2009;**63**(6):46–105.
3. Rifm T., Panel E., Belsito D., Bickers D., Bruze M., Calow P., Greim H., Hanifin JM., Rogers AE., Saurat JH., Sipes IG., Tagami H. A toxicologic and dermatologic assessment of cyclic and non-cyclic terpene alcohols when used as fragrance ingredients. *Food Chem Toxicol*. 2008;**46**. Doi: 10.1016/j.fct.2008.06.085.
4. Sirikantaramas S., Yamazaki *Æ*M. Mechanisms of resistance to self-produced toxic secondary metabolites in plants. *Phytochem Rev*. 2008;**7**:467–77. Doi: 10.1007/s11101-007-9080-2.
5. Tapia L., Torres J., Mendoza L., Urz A., Ferreira J., Pavani M., Wilkens M. Effect of 13-epi -sclareol on the bacterial respiratory chain. *Planta Med*. 2004;**70**:1058–63. Doi: 10.1055/s-2004-832647.
6. Ma M., Feng J., Li R., Chen S., Xu H. Synthesis and antifungal activity of ethers, alcohols, and iodohydrin derivatives of sclareol against phytopathogenic fungi *in vitro*.

Bioorg Med Chem Lett. 2015;**25**(14):2773–7. Doi: 10.1016/j.bmcl.2015.05.013.

7. Zhang T., Wang T., Cai P. Sclareol inhibits cell proliferation and sensitizes cells to the antiproliferative effect of bortezomib via upregulating the tumor suppressor caveolin-1 in cervical cancer cells. *Mol Med Rep*. 2017;**15**:3566–74. Doi: 10.3892/mmr.2017.6480.
8. Wang LIN., He HS., Yu HUAL., Zeng YUN., Han H., He N. Sclareol, a plant diterpene, exhibits potent antiproliferative effects via the induction of apoptosis and mitochondrial membrane potential loss in osteosarcoma cancer cells. *Mol Med*. 2015;**11**:4273–8. Doi: 10.3892/mmr.2015.3325.
9. Noori S., Hassan ZM., Salehian O. Sclareol Reduces CD4 + CD25 + FoxP3 + T-reg cells in a breast cancer model in vivo. *Iran J Immunol*. 2013;**10**(March):10–21. Doi: IJIv10i1A2.
10. Dimas K., Papadaki M., Tsimplouli C., Hatziantoniou S., Alevizopoulos K. Labd-14-ene-8,13-diol (sclareol) induces cycle arrest and apoptosis in human breast cancer cells and enhances the activity of anticancer drugs. *Biomed Pharmacother*. 2006;**60**:127–33. Doi: 10.1016/j.biopha.2006.01.003.
11. El Ridi RAF., Tallima HAM. Novel therapeutic and prevention approaches for schistosomiasis: review. *J Adv Res*. 2013;**4**(5):467–78. Doi: 10.1016/j.jare.2012.05.002.
12. CDC. Neglected Tropical Diseases. *Cdc.gov*. 2011.
13. Vale N., Gouveia MJ., Rinaldi G., Brindley PJ., Gartner F., da Costa JMC. Praziquantel for schistosomiasis: single-drug metabolism revisited, mode of action, and resistance. *Antimicrob Agents Chemother*. 2017;**61**(5):1–16. Doi: 10.1128/AAC.02582-16.
14. Doenhoff MJ., Cioli D., Utzinger J. Praziquantel: mechanisms of action, resistance and new derivatives for schistosomiasis. *Curr Opin Infect Dis*. 2008;**21**(6):659–67. Doi: 10.1097/QCO.0b013e328318978f.
15. Vinícius M., Barros O., Marcelo J., Castro D., Maria H., Rolim L., Freire G., Cerqueira GS., Regina F., Almeida DC., Maria A., Citó L., Michel P., Ferreira P., Arimatéia J., Lopes D., Melo-cavalcante AADC. Diterpenes as lead molecules against neglected tropical

diseases. *Phyther Res*. 2017;**31**:175–201. Doi: 10.1002/ptr.5749.

16. Neves B., Andrade C., Cravo P. Natural products as leads in schistosome drug discovery. *Molecules*. 2015;**20**:1872–903. Doi: 10.3390/molecules20021872.
17. de Moraes J. Natural products with antischistosomal activity. *Future Med Chem*. 2015;**7**(6):801–20. Doi: 10.4155/FMC.15.23.
18. Crusco A., Bordoni C., Chakroborty A., Whatley KCL., Whiteland H., Westwell AD., Hoffmann KF. Design, synthesis and anthelmintic activity of 7-keto-sempervirol analogues. *Eur J Med Chem*. 2018;**152**:87–100. Doi: 10.1016/j.ejmech.2018.04.032.
19. Edwards J., Brown M., Peak E., Bartholomew B., Nash RJ., Hoffmann KF. The diterpenoid 7-keto-sempervirol, derived from *Lycium chinense*, displays anthelmintic activity against both *Schistosoma mansoni* and *Fasciola hepatica*. *PLoS Negl Trop Dis*. 2015;**9**(3). Doi: 10.1371/journal.pntd.0003604.
20. Shakeel-U-Rehman., Rah B., Lone SH., Rasool RU., Farooq S., Nayak D., Chikan NA., Chakraborty S., Behl A., Mondhe DM., Goswami A., Bhat KA. Design and synthesis of antitumor heck-coupled sclareol analogues: Modulation of BH3 family members by SS-12 in autophagy and apoptotic cell death. *J Med Chem*. 2015;**58**(8):3432–44. Doi: 10.1021/jm501942m.
21. Boyle NMO., Bostro J., Sayle RA., Gill A. Using matched molecular series as a predictive tool to optimize biological activity. *J Med Chem*. 2014;**57**:2704–13. Doi: 10.1021/jm500022q.
22. Topliss JG. A manual method for applying the Hansch approach to drug design. *J Med Chem*. 1977;**20**(4):463–9. Doi: 10.1021/jm00214a001.
23. Ridi R El., Aboueldahab M., Tallima H., Salah M., Mahana N., Fawzi S., Mohamed SH., Fahmy OM. *In vitro* and *in vivo* activities of arachidonic acid against *Schistosoma mansoni* and *Schistosoma haematobium*. *Antimicrob Agents Chemother*. 2010;**54**(8):3383–9. Doi: 10.1128/AAC.00173-10.

24. Chan JD., Cupit PM., Gunaratne GS., Mccorvy JD., Yang Y., Stoltz K., Webb TR., Dosa PI., Roth BL., Abagyan R., Cunningham C., Marchant JS. The anthelmintic praziquantel is a human serotoninergic G-protein-coupled receptor ligand. *Nat Commun*. 2017;**8**(1910):1–7. Doi: 10.1038/s41467-017-02084-0.

25. Harder A., Abbink J., Andrews P., Thomas H. Praziquantel impairs the ability of exogenous serotonin to stimulate carbohydrate metabolism in intact *Schistosoma mansoni*. *Parasitol Res*. 1987;**73**:442–5.

26. Chen T., Ning D., Sun H., Li R., Shang M., Li X., Wang X., Chen W., Liang C., Li W., Mao Q., Li Y., Deng C., Wang L. Sequence analysis and molecular characterization of *Clonorchis sinensis* hexokinase , an unusual trimeric 50- kDa glucose-6-phosphate-sensitive allosteric enzyme. *PLoS One*. 2014;**9**(9). Doi: 10.1371/journal.pone.0107940.

27. Nur-e-alam M., Yousaf M., Ahmed S., Al-sheddi ES., Parveen I., Fazakerley DM., Bari A., Ghabbour HA., Threadgill MD., Whatley KCL., Hoffmann KF., Al-rehaily AJ. Neoclerodane diterpenoids from *Reehal fatima*, *Teucrium yemense*. *J Nat Prod*. 2017;**80**:1900–8. Doi: 10.1021/acs.jnatprod.7b00188.

28. Zhang J., Chung TDY., Oldenburg KR. A simple statistical parameter for use in evaluation and validation of high throughput screening assays. *J Biomol Screen*. 1999;**4**(2). Doi: 10.1177/108705719900400206.

29. Hua SK., Wang J., Chen XB., Xu ZY., Zeng BB. Scalable synthesis of methyl ent-isocopalate and its derivatives. *Tetrahedron*. 2011;**67**(6):1142–4. Doi: 10.1016/j.tet.2010.12.008.

30. Rogachev V., Löhl T., Markert T., Metz P. A short and efficient synthesis of (+) -totarol. *Arkivoc*. 2012:172–80. Doi: 10.3998/ark.5550190.0013.313.

31. Mafud AC., Silva MPN., Monteiro DC., Oliveira MF., Resende JG., Coelho ML., de Sousa DP., Mendonça RZ., Pinto PLS., Freitas RM., Mascarenhas YP., de Moraes J. Structural parameters, molecular properties, and biological evaluation of some terpenes targeting

Schistosoma mansoni parasite. *Chem Biol Interact*. 2016;**244**:129–39. Doi: 10.1016/j.cbi.2015.12.003.

32. Baptista R., Fazakerley DM., Beckmann M., Baillie L., Mur LAJ. Untargeted metabolomics reveals a new mode of action of pretomanid (PA-824). *Sci Rep*. 2018;**8**:5084. Doi: 10.1038/s41598-018-23110-1.
33. Chong J., Soufan O., Li C., Caraus I., Li S., Bourque G., Wishart DS., Xia J. MetaboAnalyst 4.0: towards more transparent and integrative metabolomics analysis. *Nucleic Acids Res*. 2018;**46**(May):486–94. Doi: 10.1093/nar/gky310.
34. Li S., Park Y., Duraisingham S., Strobel FH., Khan N., Soltow QA., Jones DP., Pulendran B. Predicting network activity from high throughput metabolomics. *PLoS Comput Biol*. 2013;**9**(7):e1003123.
35. Hosack DA., Jr GD., Sherman BT., Lane HC., Lempicki RA. Identifying biological themes within lists of genes with EASE. *Genome Biol*. 2003;**4**(10):R70. Doi: 10.1186%2Fgb-2003-4-10-r70.
36. Said V., Gawish A., El-dahab MA., Tallima H., El R. Is arachidonic acid an endoschistosomicide ? *J Adv Res*. 2018;**11**:81–9. Doi: 10.1016/j.jare.2018.01.005.
37. Barakat R., El-ela NEA., Sharaf S., Sagheer O El., Selim S., Tallima H., Bruins MJ., Hadley KB., Ridi R El. Efficacy and safety of arachidonic acid for treatment of school-age children in *Schistosoma mansoni* high-endemicity regions. *Am J Trop Med Hyg*. 2015;**92**(4):797–804. Doi: 10.4269/ajtmh.14-0675.
38. El Ridi R., Tallima H., Migliardo F. Biochemical and biophysical methodologies open the road for effective schistosomiasis therapy and vaccination. *Biochim Biophys Acta*. 2017;**1861**(1):3613–20. Doi: 10.1016/j.bbagen.2016.03.036.
39. Tallima H., Salah M., Ridi R El., Larvae SHL. *In vitro* and *in vivo* effects of unsaturated fatty acids on *Schistosoma mansoni* and *S. haematobium* lung-stage larvae. *J Parasitol*. 2005;**91**(5):1094–102.

40. Redman CA., Kennington S., Spathopoulou T., Kusel JR. Interconversion of sphingomyelin and ceramide in adult *Schistosoma mansoni*. *Mol Biochem Parasitol*. 1997;**90**:145–53. Doi: 10.1016/S0166-6851(97)00151-5.

41. Sillence DJ. Apoptosis and signalling in acid sphingomyelinase deficient cells. *BMC Cell Biol*. 2001;**2**(24). Doi: 10.1186/1471-2121-2-24.

42. Howe KL., Bolt BJ., Shafie M., Kersey P., Berriman M. WormBase ParaSite − a comprehensive resource for helminth genomics. *Mol Biochem Parasitol*. 2017;**215**:2–10. Doi: 10.1016/j.molbiopara.2016.11.005.

43. Giera M., Kaisar MMM., Derks RJE., Steenvoorden E., Kruize YCM., Hokke CH., Yazdanbakhsh M., Everts B. The *Schistosoma mansoni* lipidome : leads for immunomodulation. *Anal Chim Acta*. 2018;**1037**:107–18. Doi: 10.1016/j.aca.2017.11.058.

44. Salafsky B., Fusco AC. *Schistosoma mansoni* : A comparison of secreted vs nonsecreted eicosanoids in developing schistosomulae and adults. *Exp Parasitol*. 1987;**64**:361–7. Doi: 10.1016/0014-4894(87)90048-8.

45. Salafsky AB., Wang Y., Kevin MB., Hill H., Fusco AC., Salafsky B., Wang Y., Kevin MB., Hill H., Fusco AC. The role of prostaglandins in cercarial (*Schistosoma mansoni*) response to free fatty acids. *J Parasitol*. 1984;**70**(4):584–91.

46. Gracioso JS., Toma W., Almeida AB., Paula ACB., Brasil DSB. Gastroprotective effect of aparisthman , a diterpene isolated from *Aparisthmium cordatum*, on experimental gastric ulcer models in rats and mice. *Phytomedicine*. 2001;**8**(2):94–100. Doi: 10.1078/0944-7113-00017.

47. Parra T., Benites J., Ruiz LM., Sepulveda B., Simirgiotis M., Areche C. Gastroprotective activity of ent -beyerene derivatives in mice : effects on gastric secretion , endogenous prostaglandins and non-protein sulfhydryls. *Bioorg Med Chem Lett*. 2015;**25**(14):2813–7. Doi: 10.1016/j.bmcl.2015.04.095.

48. Brouwers JFHM., Smeenk IMB., Golde LMG Van., Tielens AGM. The incorporation ,

modification and turnover of fatty acids in adult *Schistosoma mansoni*. *Mol Biochem Parasitol*. 1997;**88**:175–85. Doi: 10.1016/S0166-6851(97)00091-1.

49. Saidur Rahman M., Mettrick DF., Podesta RB. *Schistosoma mansoni*: effects of in vitro serotonin (5-HT) on aerobic and anaerobic carbohydrate metabolism. *Exp Parasitol*. 1985;**60**:10–7. Doi: 10.1016/S0014-4894(85)80018-7.

50. Tielens AGM., van den Heuvel JM., Jan van Mazijk H., Wilsonn JE., Shoemaker CB. The 50-kDa glucose 6-phosphate-sensitive hexokinase of *Schistosoma mansoni*. *J Biol Chem*. 1994;**269**(40):24736–41.

51. Colley DG., Wikel SK. *Schistosoma mansoni*: simplified method for the production of schistosomules. *Exp Parasitol*. 1974;**35**(1):44–51.

52. Paveley RA., Mansour NR., Hallyburton I., Bleicher LS., Benn AE., Mikic I., Guidi A., Gilbert IH., Hopkins AL., Bickle QD. Whole organism high-content screening by label-free, image-based bayesian classification for parasitic diseases. *PLoS Negl Trop Dis*. 2012;**6**(7):1–11. Doi: 10.1371/journal.pntd.0001762.

53. Smithers S., Terry R. The infection of laboratory hosts with cercariae of *Schistosoma mansoni* and the recovery of the adult worms. *Parasitology*. 1965;**55**(4):695–700.

54. Ramirez B., Bickle Q., Yousif F., Fakorede F., Mouries M., Nwaka S. Schistosomes : challenges in compound screening. *Expert Opin Drug Discov*. 2007;**2**((Suppl. 1)):S53–62. Doi: 10.1517/17460441.2.S1.S53.

55. Dayeh VR., Chow SL., Schirmer K., Lynn DH., Bols NC. Evaluating the toxicity of Triton X-100 to protozoan , fish , and mammalian cells using fluorescent dyes as indicators of cell viability. *Ecotoxicol Environ Saf*. 2004;**57**:375–82. Doi: 10.1016/S0147-6513(03)00083-6.

56. Collins JJ., Wang B., Lambrus BG., Tharp ME., Iyer H., Newmark PA. Adult somatic stem cells in the human parasite *Schistosoma mansoni*. *Nature*. 2013;**494**(7438):476–9. Doi: 10.1038/nature11924.

For Table of Contents Only